*Water Resources Research*

**Supporting Information for**

# Using Inverse Modelling and Dual isotopes ($\delta^{15}N$ and $\delta^{18}O$ of $NO_3$) to Determine Sources of Nitrogen Export from a Complex Land Use Catchment

**Sri Adiyanti[1*], Yasuyuki Maruya[2], Bradley D. Eyre[3], Perrine Mangion[4], Jeffrey V. Turner[5], and Mathew R. Hipsey[1]**

[1]Aquatic Ecodynamics, School of Agriculture and Environment, The University of Western Australia, Crawley, WA, Australia 6009.

[2]Graduate School of Engineering, Kyushu University, Fukuoka, Japan.

[3] Centre for Coastal Biogeochemistry, Southern Cross University, Lismore, NSW, Australia 2480.

[4]UMR ENTROPIE, Université de La Réunion-IRD-CNRS-IFREMER-UNC, La Réunion, France

[5]CSIRO Land and Water, CELS Centre, 147 Underwood Ave, Floreat Park, WA, Australia 6014.

## Contents of this file



## Introduction

**The supporting information is provided to illustrate the detailed works involved in each step of the model framework presented in Figure 2 of the main manuscript. They are important but are not worth the space in the main manuscript as they are already known and repetitive works. The related sections are identified in the supporting information to link the information easily with the corresponding part in the manuscript.**

**The supporting information include figures outputted from a geography information system (GIS) map, MATLAB results of Markov-chain Monte Carlo simulation, and tables containing calibration results and metric calculations.**

**Text S1. Supporting information for Figure 1 of the manuscript.**

**Figure 1 of the main manuscript shows the GIS sites identification (id) number (0-50), which is used to identify the contributing DHM grids to sub-catchment flow direction in the watershed GIS toolbox processing. The corresponding sites name for each sites id is provided in Figure S1 and Table S1, with letters representing sub-catchment: w for Wararba Creek, lc for Lagoon Creek, lcds for Lagoon Creek downstram, crf for Caboolture River, ssc for Sheepstation Creek, kjc for King John Creek, etc.**

**Text S2. Supporting information for section 3.1 of the manuscript.**

**Step 1 of the model framework (Figure 2 of the main manuscript) was to simulate gridded discharges Q(x,y) using distributed hydrological model (DHM). The DHM domain is a watershed which was derived from the 25x25m$^2$ grids digital elevation model (DEM) of the basin using a GIS watershed tool. The watershed tool modelled the flow direction and flow accumulation that resulted in the derived stream network. The comparison between the derived and the reference stream network (major and minor streams) is shown in Figure S2. Hydrologic parameters utilized is provided in Table S2.**

**Text S3. Supporting information for section 3.1 of the main manuscript.**

**The value of rainfall at each grid located at (i,j), $r_n$ is the rainfall in each rainfall gauging station, and $d_{n,(i,j)}$ is the distance from a mesh (i,j) to a rainfall gauging station (n). The values of evapotranspiration were estimated using an empirical relationship of monthly air temperature and evapotranspiration, $e = 0.3046 \cdot T - 2.681$, where $T$ is the monthly mean temperature.**

**The comparison of the metrics (r, r$^2$, RMSE, Bias, NSE, RSR) between the temperature and evapotranspiration relationship shown in Figure S3 suggests that monthly temperature is a better estimator than the daily temperature.**

**Text S4. Calibration result for livestock.**

**Parameter covariance matrix resulted from MCMC calibration for livestock land use. Note, calibration for the forest land use dry period and wet period are presented in Figure 6 of the manuscript.**

**Text S5. As S4 for urban land use.**

**Text S6. Posteriors export rate (gram/ha/day) for wet period.**

**Posteriors export rates were calculated from the concentrations posteriors from MCMC calibration for the 6 land uses using Equations (9a) and (9b) presented in the manuscript. A conversion from mg to gram was applied.**

**Text S7. Sensitivity analysis.**

**We tested several ways to show the sensitivity of the model to explore the effect of the data ($NO_3$-N and $NH_4$-N concentrations and isotope abundance) to the results. The one we presented here is the one more realistic. A sensitivity analysis by arbitrarily**

**choosing the concentration and isotope abundance is not really a realistic approach, as they are land-use dependent variables at a non-mixing environment (at source/land use).**

**Sensitivity analysis was conducted to explore the effect of data distribution to the model results for the selected sampling events during wet period, i.e. $CR_5$, $CR_{11}$, $CR_{13}$. This was done by setting the data outliers of $NO_3$-N and $NH_4$-N concentrations to 20$^{th}$ percentile (lower limit) and 80$^{th}$ percentile (upper limit) and extend the data coverage using the $CR_5$, $CR_{11}$, $CR_{13}$ datasets with the following modification:**

- **Added concentration of $NO_3$-N and $NH_4$-N by 3%,**
- **Reduced flow/discharges at each location by 3%.**

**Isotope abundance $\delta^{15}N_{NO3}$ and $\delta^{18}O_{NO3}$ were unaltered. In total, a six periods dataset was utilized this exercise. Output is presented in Figure S7.**

**The comparison of the metrics between the original result and the sensitivity exercise for wet period is presented in Figure 9 of the manuscript.**

**Isotope-enabled and No-isotope mixing models evaluation metrics are detailed in Table S3.**

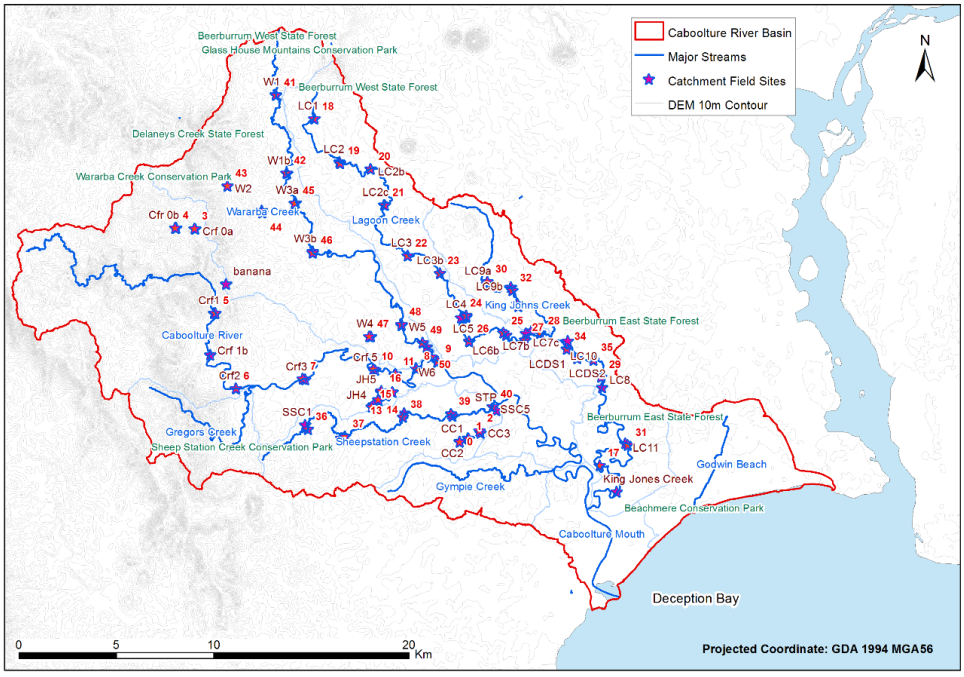


**Figure S1. Catchment sites identification number (in red) and corresponding sites name.**

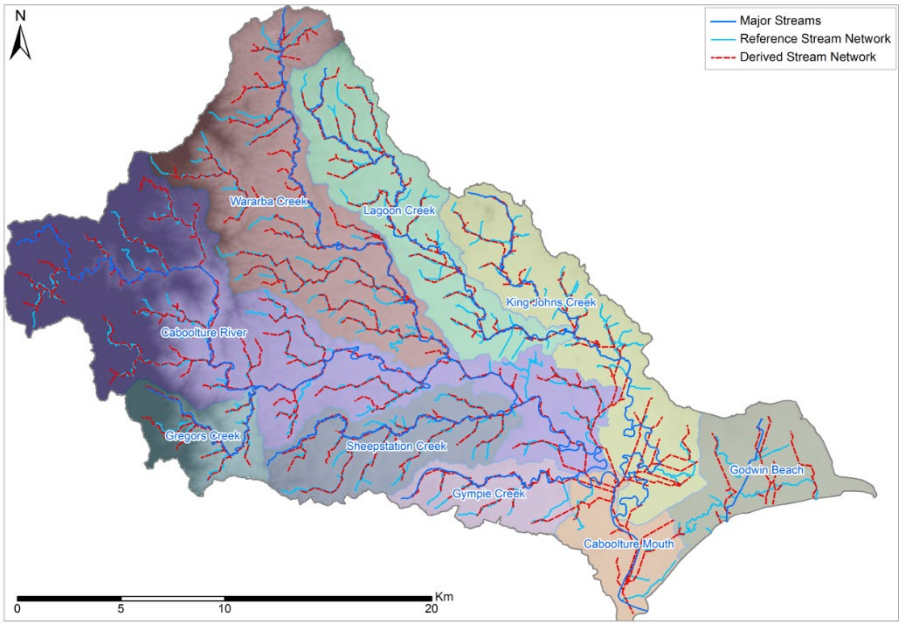


**Figure S2. Stream Network: derived (red dashed-line) and reference (light-blue solid line) stream network. Major streams were provided for comparison.**

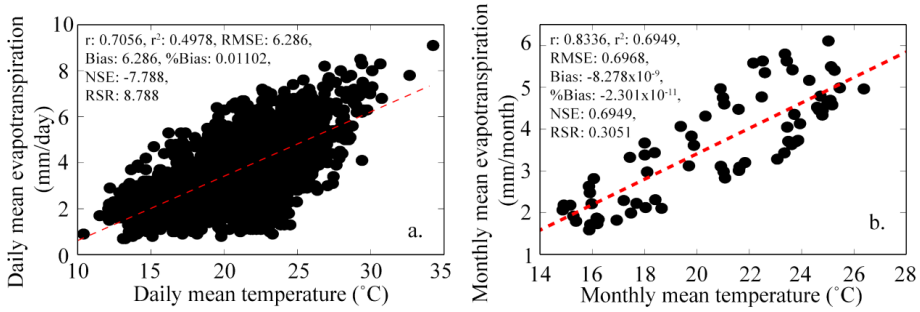


**Figure S3. Empirical relationship of temperature and evapotranspiration for daily (left) and monthly (right) resolutions.**

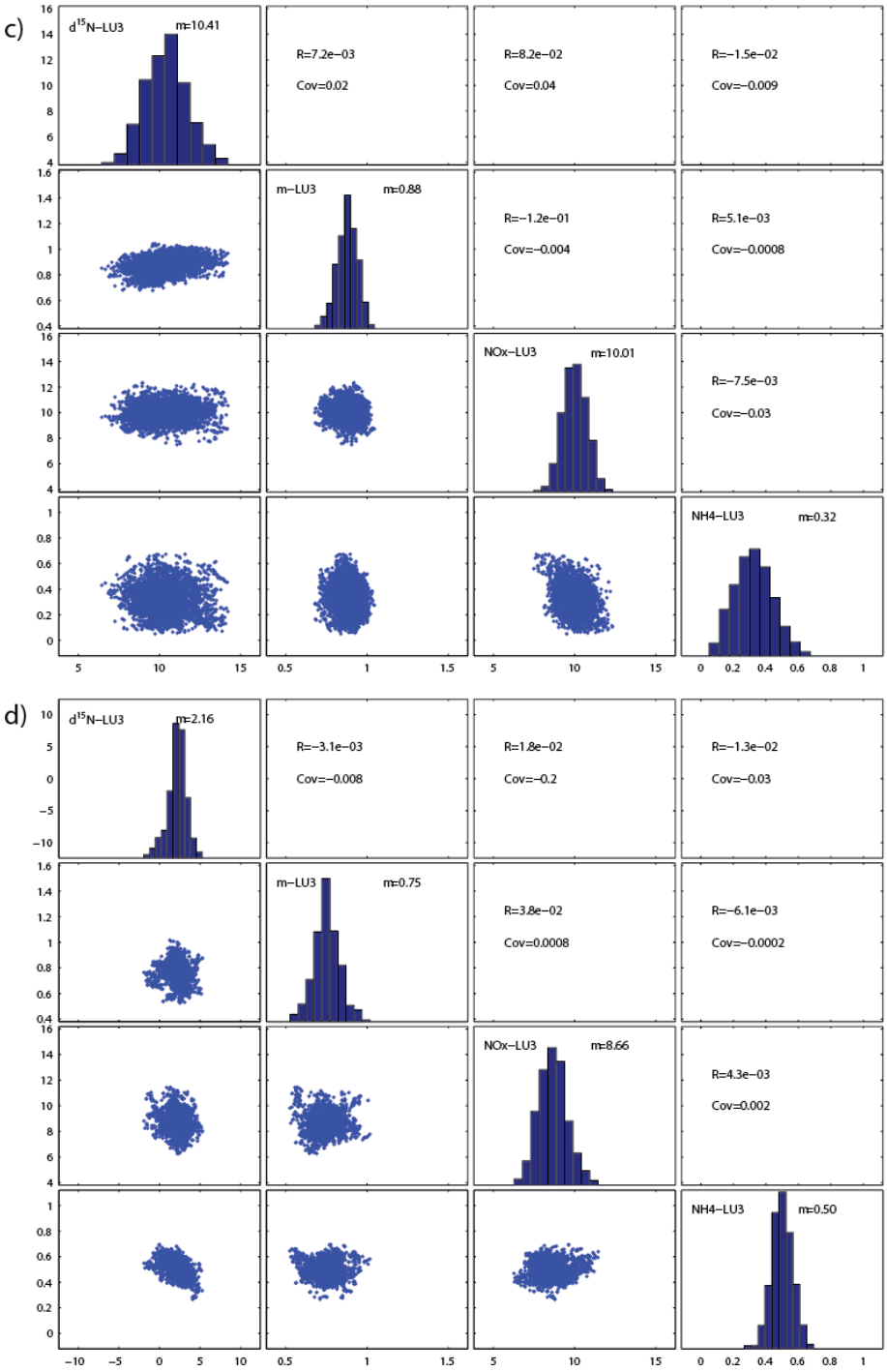


**Figure S4. Parameter covariance matrix from MCMC calibration for livestock dry (c) and wet period (d). Lower triangle: pairwise scatterplots of the 4-parameter randomizations for livestock. Upper triangle: the corresponding Pearson's correlation and Covariance coefficient. Diagonal: posterior distributions. Calibration for the forest land use dry period (a) and wet period (b) are presented in the manuscript.**

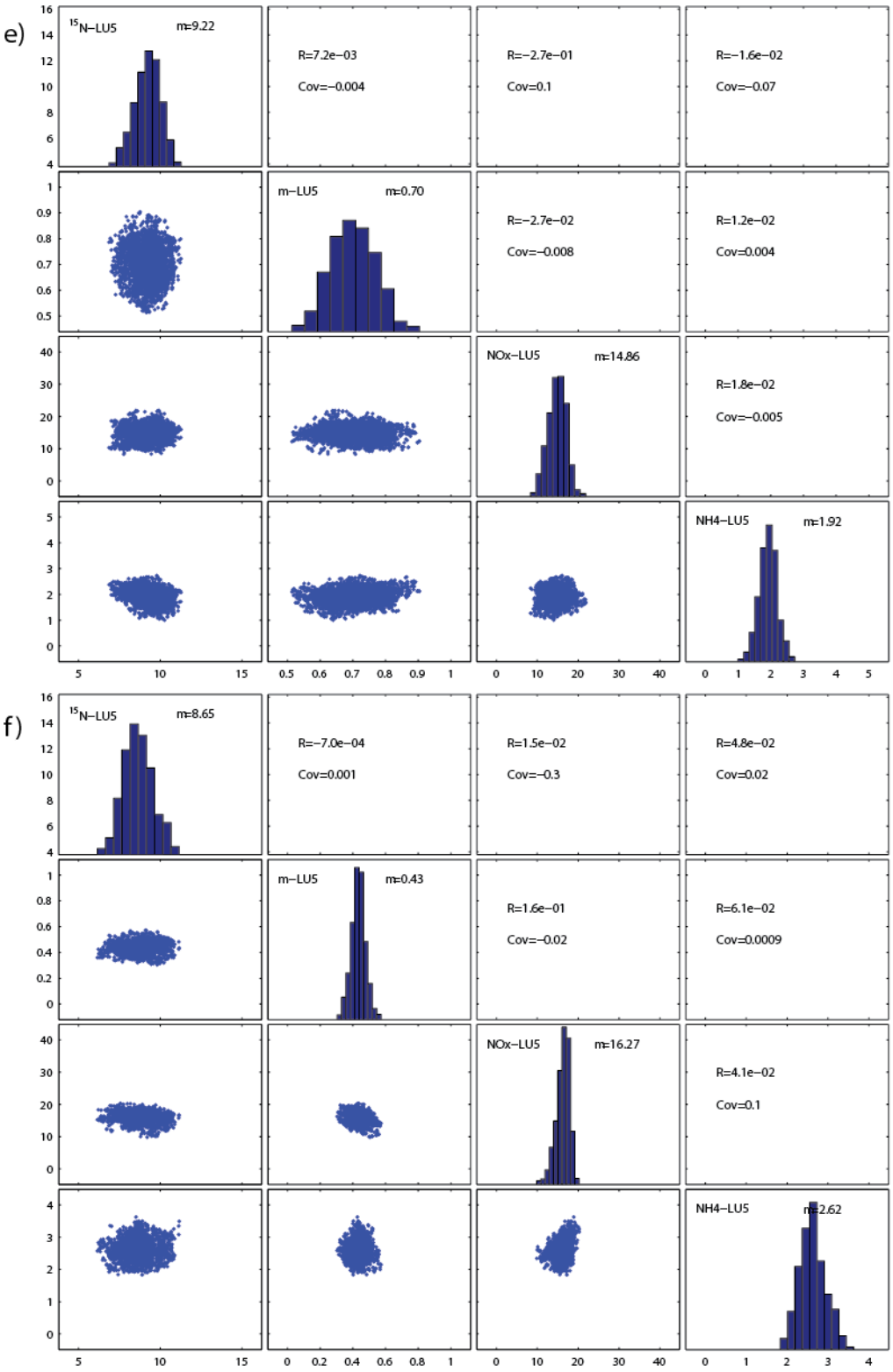


**Figure S5. As Figure S4 for urban dry period (e) and wet period (f).**

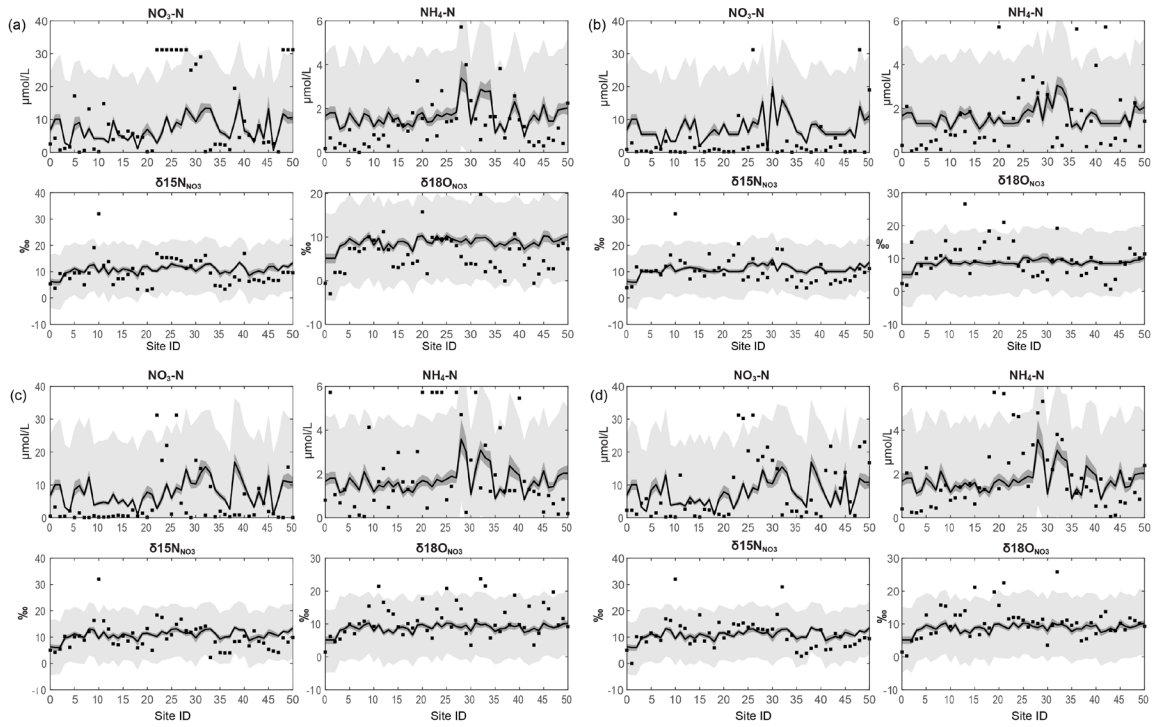


**Figure S6. Observations (■) versus median values of Bayesian mixing model for all samples $NO_3$-N, $NH_4$-N, $\delta^{15}N_{NO3}$, $\delta^{18}O_{NO3}$ for each wet period sampling campaign: (a) $CR_5$ in May 2012, (b) $CR_9$ October 2012, (c) $CR_{11}$ December 2012, (d) $CR_{13}$ February 2013. Observations (■) versus median values of Bayesian mixing model for all samples $NO_3$-N, $NH_4$-N, $\delta^{15}N_{NO3}$, $\delta^{18}O_{NO3}$. The grey zone area around the median is based on a random parameter sampling (n=1000) from posterior parameter distribution (MCMC calibration result), showing 95% confidence interval ($\mu \pm 1.96\delta$) for observations (light grey) and for model parameter (dark grey).**

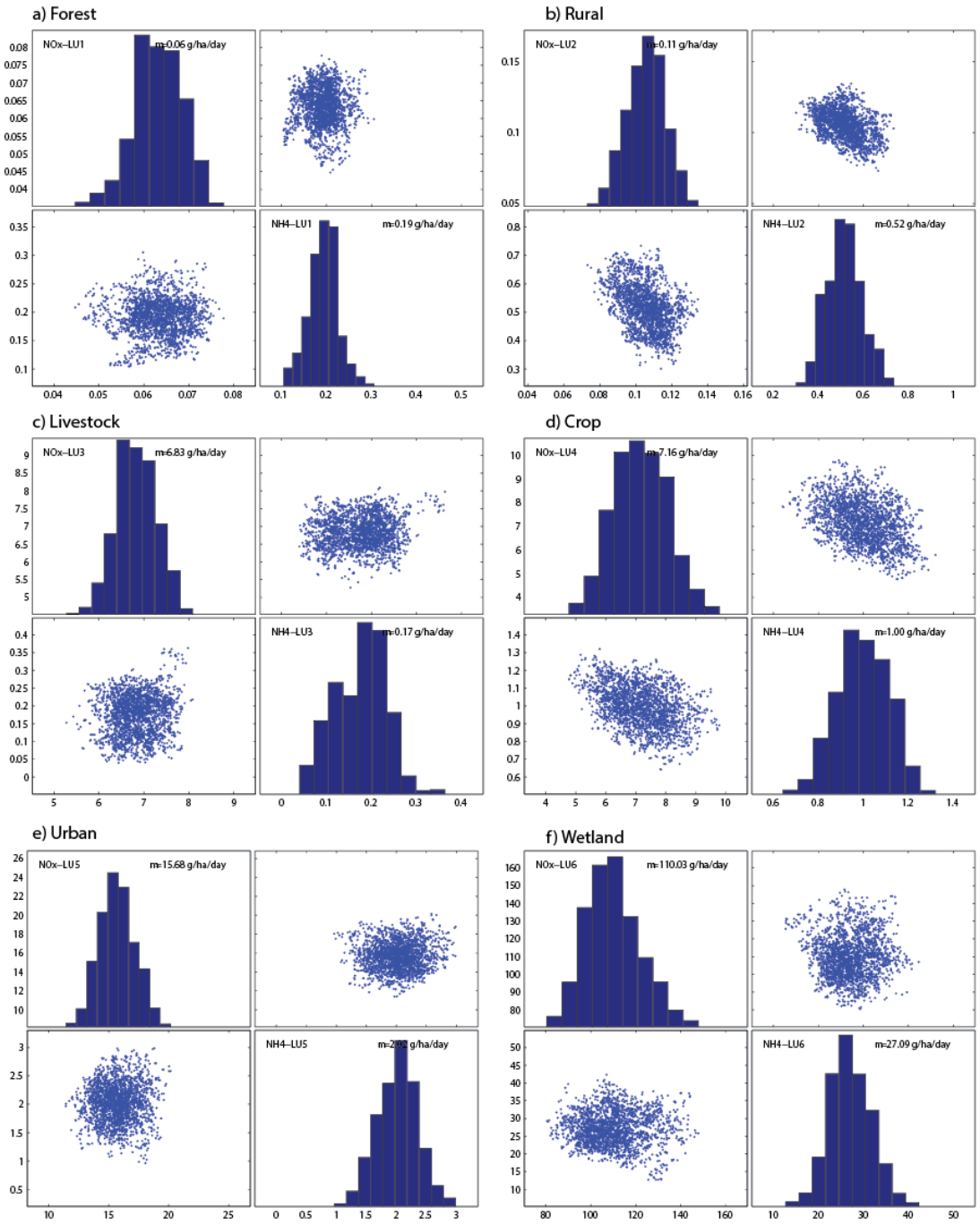


**Figure S7. Posteriors of land use specific $NO_3^-$-N and $NH_4^+$-N export rates (g/ha/day) for wet period (a conversion from mg/ha/day to g/ha/day was applied).**

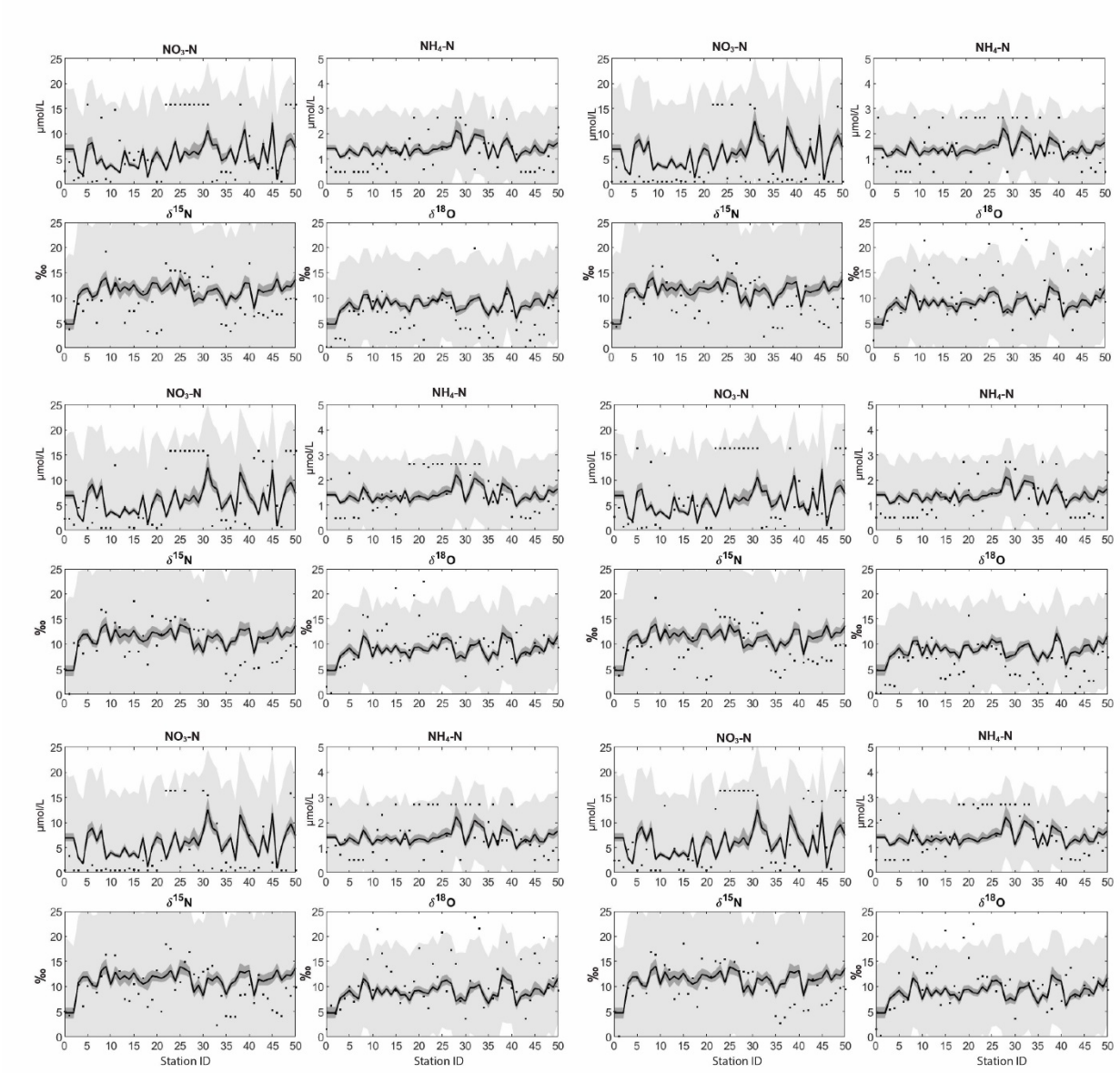


**Figure S8. Sensitivity Analysis Results. Observations (■) versus median values of Bayesian mixing model for all samples $NO_3$-N, $NH_4$-N, $\delta^{15}N_{NO3}$, $\delta^{18}O_{NO3}$ in the modified 6 datasets representing a wet period. The grey zone area around the median is based on a random parameter sampling (n=1000) from posterior parameter distribution (MCMC calibration result), showing 95% confidence interval ($\mu \pm 1.96\delta$) for observations (light grey) and for model parameter (dark grey).**

| Site ID - Name | Site ID - Name | Site ID - Name | Site ID - Name | Site ID - Name | Site ID - Name |
|---|---|---|---|---|---|
| 0 - cc1 | 9 - crf4 | 18 - lc1 | 27 - lc7c | 35 - lcds2 | 44 - w2b |
| 1 - cc2 | 10 - crf5 | 19 - lc2 | 28 - lc7b | 36 - ssc1 | 45 - w3a |
| 2 - cc3 | 11 - crf6 | 20 - lc2b | 29 - lc8 | 37 - ssc2 | 46 - w3b |
| 3 - crf0a | 12 - jh1 | 21 - lc2c | 30 - lc9a | 38 - ssc3 | 47 - w4 |
| 4 - crf0b | 13 – jh2 | 22 - lc3 | 31 - lc11 | 39 - ssc4 | 48 - w5 |
| 5 - crf2 | 14 – jh3 | 23 - lc3b | 27 - lc7c | 40 - ssc5 | 49 - w5b |
| 6 - crf2 | 15 – jh4 | 24 - lc4 | 32 - lc9b | 41 - w1 | 50 - w6 |
| 7 - crf3 | 16 - jh5 | 25 - lc6 | 33 - lc9c | 42 - w1b | |
| 8 - crf7 | 17 - kjc | 26 - lc5 | 34 - lcds1 | 43 - w2 | |

**Table S1. List of catchment sites identification number and corresponding sites name**

| Land use | $n_{slope}$ ($m^{-1/3}s$) | $k_a$ ($ms^{-1}$) | $d_a$ (m) | $d_c$ (m) | β (non-dim) |
|---|---|---|---|---|---|
| | Calibration Period: 1-31 Jan 2011 | | | | |
| Forest | 0.8024 | 0.0264 | 2.6145 | 2.9914 | 3.2946 |
| Rural | 0.0017 | 0.0004 | 0.2202 | 0.0244 | 8.1862 |
| Livestock | 0.0018 | 0.071 | 0.0051 | 0.0072 | 8.349 |
| Crops | 0.1626 | 0.0217 | 2.9773 | 1.5593 | 9.8012 |
| Urban | 0.6787 | 1.00E-17 | 0 | 0 | 1 |
| Wetland | 0.75414 | 0.7444 | 2.9702 | 0.0324 | 5.7212 |
| | Calibration Period: 1-31 Jan 2012 | | | | |
| Forest | 0.1014 | 0.0986 | 0.0462 | 0.0066 | 6.1332 |
| Rural | 0.0498 | 0.0012 | 0.0973 | 0.1882 | 3.2751 |
| Livestock | 0.7144 | 0.0005 | 1.0033 | 1.5618 | 7.3502 |
| Crops | 0.9637 | 0.0803 | 1.7485 | 0.9872 | 7.3311 |
| Urban | 0.2773 | 1.00E-17 | 0 | 0 | 1 |
| Wetland | 0.81005 | 0.9449 | 0.0637 | 0.2903 | 0.1954 |
| | Calibration Period: 1-31 Mar 2012 | | | | |
| Forest | 0.9003 | 0.075 | 1.8485 | 2.2491 | 3.2141 |
| Rural | 0.9333 | 0.0907 | 2.9018 | 2.4794 | 4.3221 |
| Livestock | 0.58 | 0.0896 | 2.7034 | 1.9394 | 3.0064 |
| Crops | 0.9772 | 0.0151 | 2.265 | 2.0865 | 6.2128 |
| Urban | 0.4796 | 1.00E-17 | 0 | 0 | 1 |
| Wetland | 0.56242 | 0.3755 | 0.0679 | 2.99 | 4.143 |
| | Calibration Period: 1 Jan -31 Mar 2012 | | | | |
| Forest | 0.6294 | 0.0766 | 0.0139 | 0.3029 | 8.8577 |
| Rural | 0.2109 | 0.0973 | 0.0076 | 0.0091 | 2.5093 |
| Livestock | 0.2755 | 0.0259 | 0.256 | 1.9999 | 5.8585 |
| Crops | 0.8168 | 0.0325 | 0.7551 | 1.995 | 7.9824 |
| Urban | 0.5762 | 1.00E-17 | 0 | 0 | 1 |
| Wetland | 0.31011 | 0.4812 | 0.0647 | 2.9161 | 4.663 |

**Table S2. Calibrated hydrological parameters for each land use from which the average parameter values were calculated from (Supporting information for section 4.2. of the main manuscript).**

| Concentration[1)] | Residual Methods | | | Correlation Methods (dimensionless) | | | |
|---|---|---|---|---|---|---|---|
| | RMSE[2)] (μM) | Bias[3)] (μM) | % Bias[4)] | r[5)] | $r^2$ | NSE[6)] | RSR[7)] |
| **Isotope-enabled mixing model: Wet Period** | | | | | | | |
| $NO_3^-$-N (μM) | 109 | -0.39 | -5.8 | 0.53 | 0.28 | 0.27 | 0.85 |
| $NH_4^+$-N (μM) | 19 | 0.11 | 6.2 | 0.47 | 0.22 | 0.22 | 0.88 |
| **No-isotope mixing model: Wet Period** | | | | | | | |
| $NO_3^-$-N (μM) | 124 | -0.70 | -10 | 0.29 | 0.08 | 0.07 | 0.97 |
| $NH_4^+$-N (μM) | 21 | 0.06 | 3.7 | 0.25 | 0.06 | 0.04 | 0.98 |
| **Isotope-enabled mixing model: Dry Period** | | | | | | | |
| $NO_3^-$-N (μM) | 108 | 4.9 | 53 | 0.39 | 0.15 | -0.03 | 0.98 |
| $NH_4^+$-N (μM) | 13 | 0.42 | 23 | 0.30 | 0.10 | 0.09 | 0.99 |
| **No-isotope mixing model: Dry Period** | | | | | | | |
| $NO_3^-$-N (μM) | 122 | 5.14 | 55 | 0.09 | 0.01 | -0.22 | 1.11 |
| $NH_4^+$-N (μM) | 14 | 0.39 | 23 | 0.29 | 0.08 | 0.01 | 1.00 |
| **Range values** | [0 ∞] | [-∞ ∞] | [-100 100] | [-1 1] | [0 1] | [0 1] | [0 ∞] |
| **Ideal value** | 0 | 0 | 0 | 1 | 1 | 1 | 0 |

[1)] **Concentration at each sampling sites; refer to Equations 7(c) and 7(d).**

[2)] **Root Mean Square Error:** $RMSE = \sqrt{1/n \sum_{i=1}^{n} \left(Y_{obs,i} - Y_{sim,i}\right)^2}$

[3)] **Bias** $= 1/n \sum_{i=1}^{n} (Y_{obs,i} - Y_{sim,i})$**. Positive value indicates model underestimation bias, and vice versa.**

[4)] **%Bias** $= \sum_{i=1}^{n} (Y_{obs,i} - Y_{sim,i}) \,/\, \sum_{i=1}^{n} \left(Y_{obs,i}\right) * 100$

[5)] **Pearson correlation (r) and coefficient determination ($r^2$):** $r = \frac{n\left(\sum_{i=1}^{n} Y_{obs,i} . Y_{sim,i}\right) - \left(\sum_{i=1}^{n} Y_{obs,i}\right) . \left(\sum_{i=1}^{n} Y_{sim,i}\right)}{\sqrt{\left[n . \sum_{i=1}^{n} Y_{obs,i}^2 - \left(\sum_{i=1}^{n} Y_{obs,i}\right)^2\right]} \sqrt{\left[n . \sum_{i=1}^{n} Y_{sim,i}^2 - \left(\sum_{i=1}^{n} Y_{sim,i}\right)^2\right]}}$

[6)] **Nash-Sutcliffe efficiency (NSE)(Nash and Sutcliffe, 1970):** $NSE = 1 - \left[\frac{\sum_{i=1}^{n} \left(Y_{obs,i} - Y_{sim,i}\right)^2}{\sum_{i}^{n} \left(Y_{obs,i} - \overline{Y_{obs}}\right)^2}\right]$

[7)] **RSR is a normalized RMSE,** $RSR = \frac{RMSE}{STDEV_{obs}} = \frac{\sqrt{\frac{1}{n} \sum_{i=1}^{n} \left(Y_{obs,i} - Y_{sim,i}\right)^2}}{\sqrt{\frac{1}{n} \sum_{i=1}^{n} \left(Y_{obs,i} - \overline{Y_{obs}}\right)^2}}$

**Table S3. Isotope-enabled and No-isotope mixing models evaluation metrics (Supporting information for section 4.2. of the manuscript)**